

## Magnetic phase transition in $\text{La}_{1-x}(\text{Ca,Sr})_x(\text{Mn,Co})\text{O}_3$ perovskites

J. Mira and J. Rivas

Departamento de Física Aplicada, Universidade de Santiago, E-15706 Santiago de Compostela, Spain

### ABSTRACT

We review some recent results concerning the ferromagnetic-to-paramagnetic phase transition found in materials with perovskite structure in the form  $\text{La}_{1-x}\text{A}_x\text{MO}_3$  (A= divalent alkali, M=Mn, Co). This critical point has associated a very rich variety of physical phenomena, among wick is colossal magnetoresistance (CMR). In mixed-valence manganites of formula  $\text{La}_{2/3}\text{Ca}_{1/3}\text{MnO}_3$  the magnetic phase transition is of first order, and CMR, anomalous volume changes, metal-insulator transitions and other effects are found; in contrast with  $\text{La}_{2/3}\text{Sr}_{1/3}\text{MnO}_3$  and Co-based perovskites, where this is not observed and the phase transition is of second order. It allows us to clasify this type of oxides in two groups attending to the associated phenomena at the critical point. The transtion from itinerant to polaronic conduction in cobaltites is also analyzed.



Transworld  
Research Network  
T.C. 36/248(1),  
Trivandrum-695 008, India.

## 1. INTRODUCTION

The magnetic and electronic properties of LMO<sub>3</sub> materials (L= lanthanide, M= transition metal), crystallizing in the perovskite structure, started to be studied systematically about 50 years ago. The pioneers in the field, Jonker and van Santen, soon realized in M= Mn perovskites that the system provides a nice opportunity to observe correlations between structural, electrical and magnetic properties by doping with divalent atoms at the L site [1]. In the mid-50's Wollan and Koehler determined the magnetic phase diagram of La<sub>1-x</sub>Ca<sub>x</sub>MnO<sub>3</sub> [2], interpreted by Goodenough [3] in terms of the charge and orbital ordering of Mn-O bonds. They found in certain ranges a ferromagnetic phase with associated electronic conductivity, indicating a direct correlation between electron transport and magnetic properties. The finding of ferromagnetism in oxides with high conductivity motivated theoretical works by Zener [4], Anderson and Hasegawa [5] and de Gennes [6], that led to the interpretation of the observations in terms of the so called double-exchange (DE) interaction. Within the double exchange scenario in manganites, a coexistence of Mn<sup>3+</sup> and Mn<sup>4+</sup> species is assumed, so that conducting electrons carry electric charge in a common *d* band, thus resulting in high conductivity. Conducting electrons do not change their spin during motion, and Mn ions align their magnetic moments parallel to the spin of the itinerant electrons through *s-d* interaction. The final effect is a ferromagnetic ordering. The transfer of itinerant electrons is dependent on the relative angles formed by the magnetic moments of both Mn ions.

Despite the rich physics of these materials, it was not till the 90's when the research activity increased considerably, due to the discovery of a very high magnetoresistive effect [7, 8] (i.e. an enormous change of electrical resistivity under the application of an external magnetic

field, which, obviously, has very promising technological applications), labelled "colossal" by Jin et al. [9]. Actually, the works of von Helmolt et al. [7], Chahara et al. [8] and Jin et al. [9] were not the first reports on the finding of high magnetoresistance in perovskites. There had been some in the late 60's [10, 11], but the ones in the 90's impacted the scientific community because of appearing just in a moment in which the field of magnetoresistive devices had been revitalized after the finding by Baibich et al. [12] of giant MR in Fe-Cr multilayers. Also, after the shocking years of high temperature superconductivity (HTCS) [13] a lot of groups were well prepared for the study of these compounds, with many similarities with HTCS's. Some new 3d transition metal oxides were soon shown to display large MR, associated with the ferromagnetic-paramagnetic (FM-PM) phase transition, which in some cases coincides with a metal-insulator one. It is near this critical point where the enormous MR is found. Therefore the relationship between both phenomena seems plausible. Correlations between magnetization and resistivity were soon detected [14]. In a first moment, CMR was explained just within a double exchange formalism [15], taking into account that an external applied magnetic field aligns the moments of the transition metal ions, thus enabling electronic conduction. Nevertheless, Millis, Littlewood and Shraiman detected a lack of consistence between the orders of magnitude calculated for CMR in a pure double-exchange model and those measured experimentally [16]. Millis, Shraiman and Müller pointed out the inclusion of lattice effects to compensate the difference [17]. The role of electron-phonon interactions [18] has been confirmed by several experiments [19,20], even by their effects on the magnetic interaction [21]. In a small angle neutron scattering (SANS) experiment, de Teresa et al. [22] found evidence for magnetic polarons (i.e. charge carriers accompanied by a localized and

magnetically polarized distortion of the surrounding crystal lattice) and invoked them as explanation of CMR. The basis of their reasoning lies on the response of these magnetic polarons to an applied magnetic field, more exactly, such polarons grow in size under magnetic field [22], enabling electrical conduction.

From the previous paragraphs it is clear the importance of the ferromagnetic-to-paramagnetic phase transition of these perovskites. In this article we review the last results of our group and collaborators in the topic. The first part is devoted to ferromagnetic manganites, discussing about the first- or second-order character of their magnetic phase transitions. It is followed by a discussion about the behaviour of electrical conductivity above the phase transition, explored by thermopower measurements. We finish with an analysis of ferromagnetic Co-based perovskites, both at their Curie temperature as well as at temperatures above the ferromagnetic phase.

## 2. DO ALL THE FERROMAGNETIC MANGANITES EXHIBIT A FIRST-ORDER TRANSITION AT $T_C$ ?

Mn-based perovskites  $(L,A)MnO_3$  ( $L$ =lanthanide,  $A$ =alkaline earth), present, at certain doping ranges, a ferromagnetic phase below a Curie temperature,  $T_C$  [23]. The most studied cases are those of  $L=La$  with  $A=Ca$  and  $Sr$ .  $La_{1-x}Ca_xMnO_3$  is ferromagnetic and insulator for low Ca doping and, for  $0.20 \leq x \leq 0.50$ , a ferromagnetic metal [23,24]. For  $A=Sr$  the ferromagnetic phase is found for  $x \geq 0.10$ , which for  $x \leq 0.17$  turns also into metallic [25]. In both, the maximum  $T_C$  takes place for  $x=1/3$ , which means a ratio  $Mn^{3+}/Mn^{4+}=2$ . The maximum in  $T_C$  means that the ferromagnetic (double exchange?) interaction is optimized at such doping value, which is not logical,

because in principle one expects a maximum double exchange effect for  $x=0.5$ . Besides, for  $x=2/3$ , i. e.  $Mn^{4+}/Mn^{3+}=2$ , the behaviour should be the same as for  $x=1/3$ , and it is not. All these facts reveal that there could be extra terms in the magnetic interaction.

In  $(La,Ca)MnO_3$  several rich phenomena gather at the critical point: in addition to the ferromagnetic transition the material changes from metallic to insulator [23], anomalous thermal lattice expansions are measured [26] and, specially, huge changes of electrical resistivity under an external magnetic field (magnetoresistance) are detected [9]. The phenomenon, as commented in the introduction, was labelled by Jin et al. [9] as "colossal", and has been the decisive reason for the renaissance of the research activity on these materials since 1993. It is thus evident that  $T_C$  is the first point to inspect if we are willing to discover the physics of the manganites. In the particular case of  $La_{2/3}Ca_{1/3}MnO_3$ , the large volume changes and the thermal hysteresis in resistivity around  $T_C$  led to think that a first-order transition was taking place. Lynn et al. found later, by neutron scattering investigations [27], that the ferromagnetic transition was "unconventional". In a previous work Hwang et al. [24] had proposed that in  $La_{0.7}A_{0.3}MnO_3$  an abrupt change of the matrix element describing the electron hopping between Mn sites would cause an abrupt change in the double exchange coupling value and might be responsible for a first-order transition. Archibald, Zhou and Goodenough [28] generalized the conclusion to  $La_{0.7}A_{0.3}MnO_3$  orthomanganites on the basis of a transition from polaronic to itinerant electrons, that would be reflected in a compensating discontinuous change in the mean potential energy, explaining a first-order decrease in the mean Mn-O bond length.

Nevertheless, despite the abovementioned contributions, some groups started to suggest

that the transition might be of second-order [29]. Concretely, Lofland et al. [30], by microwave absorption techniques, arrived to the conclusion that the ferromagnetic-to-paramagnetic transition of  $\text{La}_{0.7}\text{Sr}_{0.3}\text{MnO}_3$  is continuous, of second-order. The apparent contradiction motivates an analysis of the phase transition in mixed  $\text{La}_{2/3}(\text{Ca,Sr})_{1/3}\text{MnO}_3$  in order to detect if the different results are caused by interpretation errors or if there is any factor changing when passing from  $A = \text{Sr}$  to  $\text{Ca}$  [31]. The data to be obtained are the character of the phase transition: of first- or second-order. To do this, a criterion given by Banerjee is used [32]. It allows the determination of the order of a magnetic transition. Banerjee detected the essential similarity between the Landau-Lifshitz [33] and Bean-Rodbell [34] criteria and condensed them into one that provides a tool to distinguish first order magnetic transitions from second order ones by purely magnetic methods. It consists on the observation of the slope of isotherm plots of  $H/M$  versus  $M^2$ , being  $M$  the experimentally observed magnetization and  $H$  the magnetic field. A positive or negative slope indicates a second order or first order transition respectively. We have applied this to two compounds that have been at the center of the controversy: Besides, intermediate compositions have been analyzed, namely  $\text{La}_{2/3}(\text{Ca}_{1-x}\text{Sr}_x)_{1/3}\text{MnO}_3$  materials with  $x=0, 0.05, 0.15, 0.25$  and  $1$ , in order to observe the tendency between the two end members of the series. We note that in some of the literature a mention to  $\text{La}_{0.7}\text{A}_{0.3}\text{MnO}_3$  instead of  $\text{La}_{2/3}\text{A}_{1/3}\text{MnO}_3$  is made. In any case, in the framework of the phase diagram proposed by Urushibara et al. [25] for  $\text{La}_{1-x}\text{Sr}_x\text{MnO}_3$ , it is clear that variations from  $x=0.30$  to  $x=0.33$  are negligible, and the conclusions obtained here for  $x=0.30$  are valid for  $x=0.33$ . The same argument serves for the  $x=0.30$  and  $x=0.33$  Ca-doped samples [23].

Samples  $\text{La}_{2/3}(\text{Ca}_{1-x}\text{Sr}_x)_{1/3}\text{MnO}_3$ , with  $x=0,$

$0.05, 0.15, 0.25$  and  $1$ , were prepared by solid state reaction of  $\text{La}_2\text{O}_3, \text{CaO}, \text{SrCO}_3, \text{MnO}_2$  and  $\text{MnO}$  (at least 99.995 % in purity), which were heated in air in two steps (1100 C, 70 hours; 1200 C, 27 hours) and pressed into disks. The temperature was slowly ramped at 5 C/min, and cooled down to room temperature at 2 C/min. Intermediate grindings were made. Pellets were finally annealed at 1300 C for 100 hours, with an intermediate grinding at 30 hours. The nominal oxygen content was near the stoichiometric value as determined by iodometric analysis (for example  $3 \pm \delta = 2.965(3)$  and  $2.98(2)$  for  $\text{LaSrMnO}$  and  $\text{LaCaMnO}$  respectively). X-ray powder patterns were collected at room temperature using a Philips PW1710 diffractometer, working with  $\text{CuK}\alpha$  radiation. The lattice parameters for the end members of the series, derived by Rietveld analysis, are in agreement with those reported in the literature. Electron Spin Resonance (ESR) spectra of the samples were taken at 9.5GHz (X-band) between 110 and 700 K with a Bruker ESP-300 and a Bruker EMX spectrometer. The small linewidth observed in our samples is a signature of the good quality and homogeneity of the material [35]. Magnetic measurements were performed with a Quantum Design SQUID and a DMS-1660 Vibrating Sample Magnetometer (VSM).

Low field magnetization versus temperature was first measured for both end members of the series, in order to have an estimation of the transition temperatures. The results are presented in Fig. 1 and from them we extract Curie temperatures of the order of 260 K for  $\text{La}_{2/3}\text{Ca}_{1/3}\text{MnO}_3$  and 370 K for  $\text{La}_{2/3}\text{Sr}_{1/3}\text{MnO}_3$ , both in agreement with data reported in previous literature [27,30]. In order to apply the Banerjee criterion we have measured initial magnetization isotherms in the vicinity of the critical points. Before each run, samples were heated above their  $T_C$  and cooled to the measuring temperature under zero field, in order to ensure a perfect

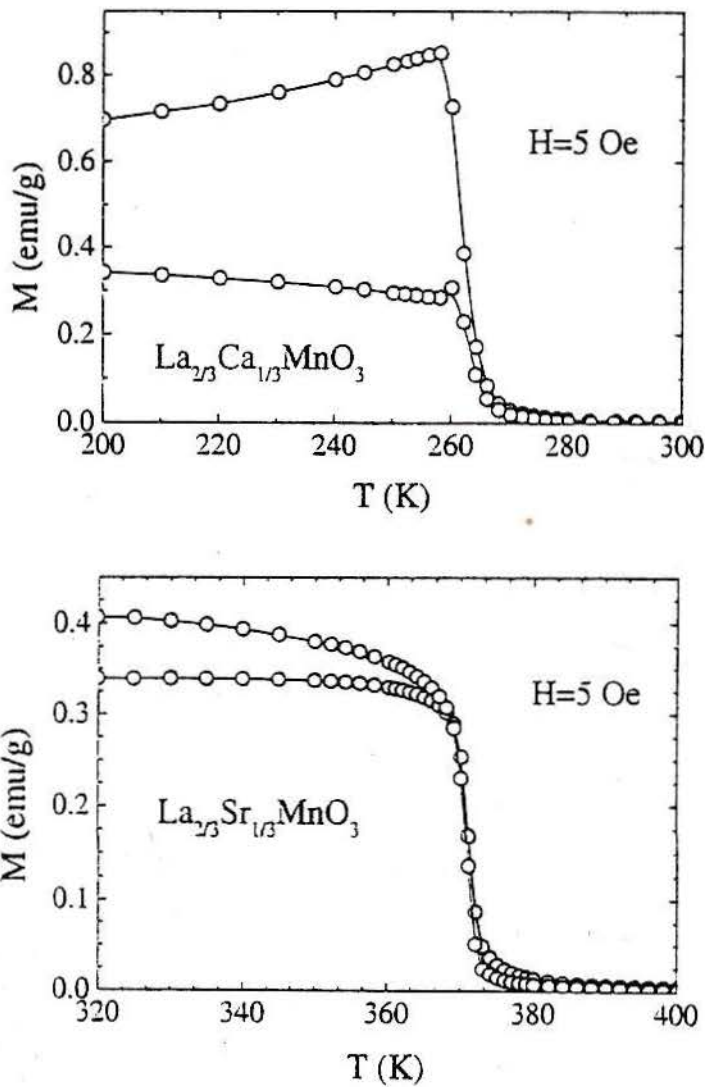


Figure 1. Magnetization versus temperature for  $\text{La}_{2/3}\text{Ca}_{1/3}\text{MnO}_3$  and  $\text{La}_{2/3}\text{Sr}_{1/3}\text{MnO}_3$  under an applied magnetic field of 5 Oe. (J. Mira et al. [31]).

demagnetization of the samples. Fig. 2(a) shows the results for  $\text{La}_{2/3}\text{Ca}_{1/3}\text{MnO}_3$ . The first characteristic that calls our attention is the peculiar behaviour of the curves at intermediate

fields, where a decrease of slope followed by an increase is observed. This behaviour near the critical point was observed by Bean and Rodbell in  $\text{MnAs}$  [34] (which presents a first-

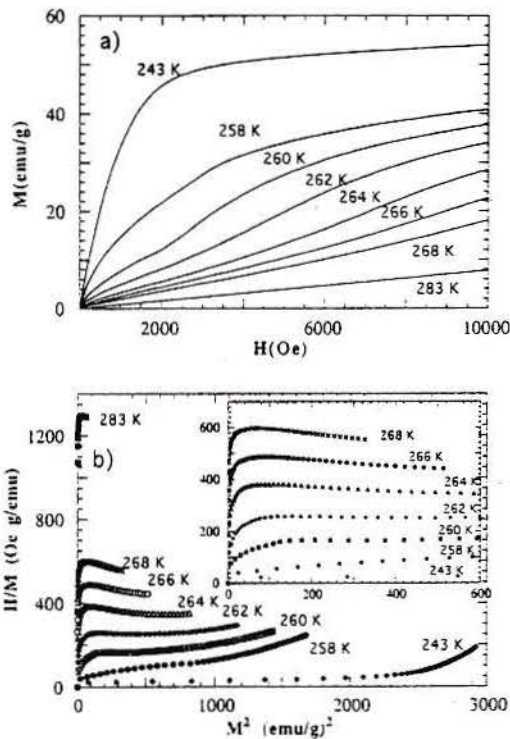


Figure 2. (a) Magnetization versus magnetic field isotherms for  $\text{La}_{2/3}\text{Ca}_{1/3}\text{MnO}_3$  in the vicinity of its  $T_C$ . Note the anomalies of slope at intermediate fields for isotherms between 258 and 268 K. (b)  $H/M$  vs.  $M^2$  plot of the above isotherms. It is clear the negative sign of the slope for some temperatures. The inset shows the detail for small values of  $M^2$ . (J. Mira et al. [31]).

order transition at its Curie temperature) and used by Banerjee to test his criterion [32]. In Fig. 2(b) we apply it and obtain that  $H/M$  vs.  $M^2$  isotherms between 260 and 268 K present negative slopes in some parts, which according to the criterion used here is an indication of the first-order character of the transition. A similar change of slope in  $M$  vs.  $H$  isotherms has been observed recently in the layered manganite

$\text{La}_{1.2}\text{Sr}_{1.8}\text{Mn}_2\text{O}_7$  [36] at the first-order phase transition point from a ferromagnetic to a canted state [37] which exhibits colossal magnetoresistance.

When the same measurements in  $\text{La}_{2/3}\text{Sr}_{1/3}\text{MnO}_3$  are done it is seen that the isotherms (Fig. 3(a)) do not display the anomalous change of slope of the previous case. This difference is more clearly seen in the  $H/M$  vs.  $M^2$  plots of Fig. 3(b) where a positive slope for all the  $M^2$  range is present.

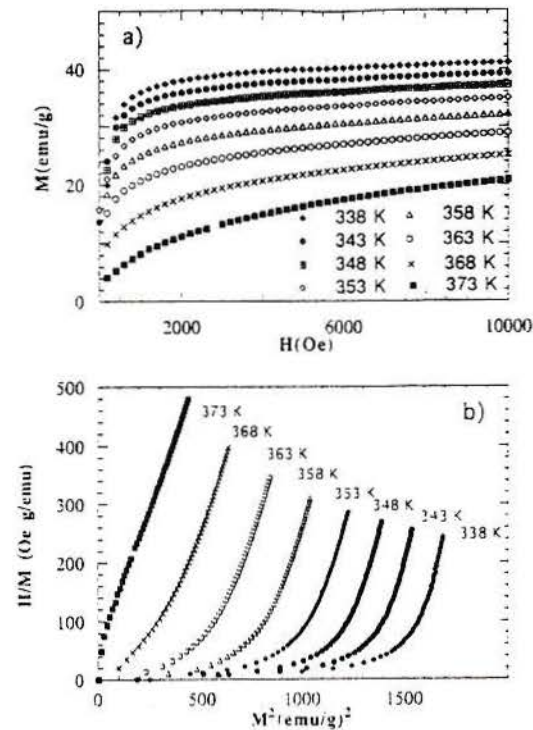


Figure 3. (a) Magnetization versus magnetic field isotherms for  $\text{La}_{2/3}\text{Sr}_{1/3}\text{MnO}_3$  in the vicinity of its  $T_C$ . (b)  $H/M$  vs.  $M^2$  plot for such isotherms. The slope is always positive, denoting the second order character of the phase transition. (J. Mira et al. [31]).

Substitution of Ca by Sr causes an increase of  $T_C$  (Fig. 4(a)) as well as a decrease of the low field magnetization and a reduction of the differences between zero field cooled and field cooled  $M$  vs.  $T$  curves. It is detected that the character of the transition is very sensitive to Sr-doping. Inspecting the Banerjee plot of Fig. 4(b) it can be seen that for  $x=0.05$  the material presents still a first order phase transition at  $T_C$ , but, attending to the slopes, such character is weaker than in  $\text{La}_{2/3}\text{Ca}_{1/3}\text{MnO}_3$ . In the case of  $\text{La}_{2/3}(\text{Ca}_{0.85}\text{Sr}_{0.15})_{1/3}\text{MnO}_3$  the phase transition is already a second-order one (Fig. 4(c)).

When the properties of the end members of the series are compared, one of the main qualitative differences is that the transition at  $T_C$  is not accompanied by a metal-insulator transition in  $\text{La}_{2/3}\text{Sr}_{1/3}\text{MnO}_3$  [25]. Nevertheless, that does not seem to be a significative effect:  $\text{La}_{0.8}\text{Sr}_{0.2}\text{MnO}_3$  does show a metal-insulator transition near  $T_C$  [25], and inspecting the Arrott plots [38] given by Lofland et al. [39] and Mohan et al. [40] it is clear that the magnetic transition is also of second-order for this composition.

From this part it is concluded, using a criterion given by Banerjee, that although  $\text{La}_{2/3}\text{Ca}_{1/3}\text{MnO}_3$  exhibits a first-order transition at  $T_C$ ,  $\text{La}_{2/3}\text{Sr}_{1/3}\text{MnO}_3$  does not. Therefore, the existence of a first-order transition for the  $\text{L}_{2/3}\text{A}_{1/3}\text{MnO}_3$  orthomanganites, irrespective of the identity of L or A cannot be stated [31]. The nature of the ferromagnetic-paramagnetic phase transition of CMR systems has been the concern of some experiments, recently also in layered manganites [41] but clear conclusions could not be drawn. Eventual attempts in the search for connections between colossal magnetoresistance and first-order transitions should be aware of the results presented here, for example in those trying to relate the behaviour of the correlation length at  $T_C$  with

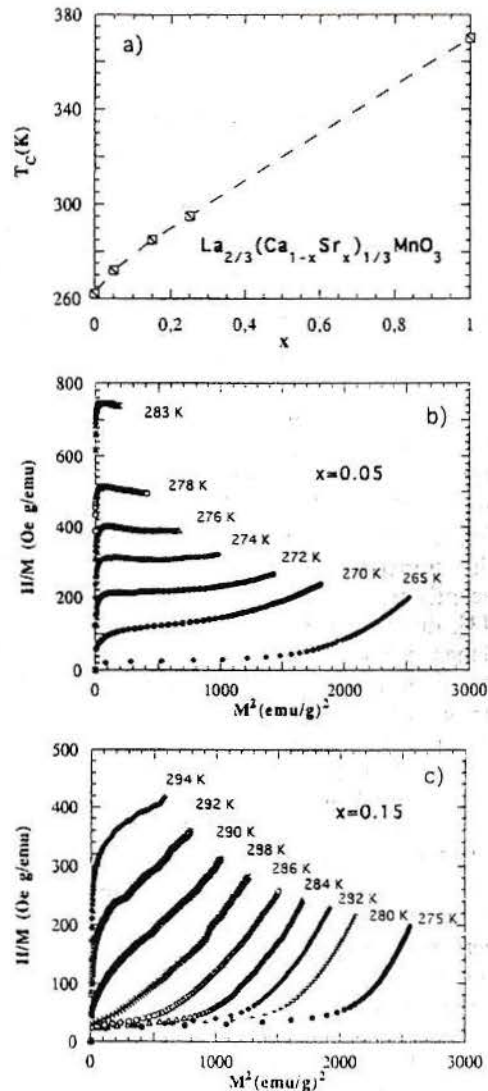


Figure 4. (a) Dependence of the Curie temperature,  $T_C$ , on the Sr-doping degree,  $x$ . (b)  $H/M$  vs.  $M^2$  plots of isotherms in the vicinity of the Curie point of  $\text{La}_{2/3}(\text{Ca}_{0.95}\text{Sr}_{0.05})_{1/3}\text{MnO}_3$ . (c)  $H/M$  vs.  $M^2$  plots of isotherms in the vicinity of the Curie point of  $\text{La}_{2/3}(\text{Ca}_{0.85}\text{Sr}_{0.15})_{1/3}\text{MnO}_3$ . (J. Mira et al. [31]).

the formation of magnetic polarons [22].

### 3. CRYSTAL SYMMETRY AND ELECTRICAL CONDUCTIVITY ABOVE THE CRITICAL POINT

In the previous section it was pointed out that ferromagnetic manganites do not behave in the same way from a magnetic point of view, attending to their phase transition. And what about the electrical properties? Above  $T_C$  there are also differences:  $\text{La}_{1-x}\text{Ca}_x\text{MnO}_3$  changes from insulator to metallic conduction for  $x > 0.25$  [23,42], whereas  $\text{La}_{1-x}\text{Sr}_x\text{MnO}_3$  does not in the ferromagnetic doping range [25,42]. But there could be another changes simultaneously to the change from first- to second-order character of the phase transition. The transport properties have been found recently to be anisotropic in layered materials [43], due to the decoupling of in-plane (MnO planes) and out-of-plane transport behavior. In the prototypical CMR  $\text{La}_{2/3}\text{Sr}_{1/3}\text{MnO}_3$  manganites, their pseudo-cubic perovskite structure should make difficult to observe any anisotropy in electrical conduction. Recently, Zeng and Wong reported the observation of anisotropic transport properties of  $\text{LaCaMnO}$  thin films [44]. But, it has been recently shown [45] that this anisotropic behaviour is not a general property of Mn-based perovskites, but there are two conduction regimes, isotropic and anisotropic, related to the crystal structure of the considered material.

For this purpose two high-quality  $\text{Pr}_{2/3}\text{Sr}_{1/3}\text{MnO}_3$  and  $\text{La}_{2/3}\text{Sr}_{1/3}\text{MnO}_3$  single crystals were available. They were prepared with the same technique used in [46]. In Fig. 5 the x-ray pattern of the  $\text{Pr}_{2/3}\text{Sr}_{1/3}\text{MnO}_3$  is shown. The analysis indicated high purity and almost perfect single crystal structure, with a rocking curve full width at half maximum of 0.04 degrees. Deviations from the expected orientation were found to be lower than 0.5 degrees. Special care was taken in order to

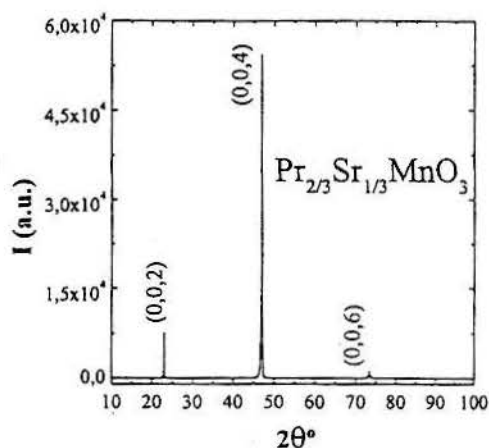


Figure 5. X-ray diffraction pattern of the  $\text{Pr}_{2/3}\text{Sr}_{1/3}\text{MnO}_3$  single crystal. Only sharp (002), (004), and (006) peaks are observed, demonstrating the high quality of the crystal. (J. Mira et al. [45]).

ensure that no mixture of phases is present in the crystals due to the synthesis route. For this reason room temperature x-ray diffraction patterns of powdered samples were recorded and adjusted by the Rietveld method.  $\text{La}_{2/3}\text{Sr}_{1/3}\text{MnO}_3$  is rhombohedral (R-3c, spatial group 167) whereas  $\text{Pr}_{2/3}\text{Sr}_{1/3}\text{MnO}_3$  was found to be orthorhombic (Pbnm, spatial group 62). Long-time high resolution scans were performed between the (0,0,2) and (0,0,4) peaks, showing no presence of twinned structures. Bond distances and angles are summarized in Table 1. DC-magnetization measurements were done in order to estimate the Curie temperatures,  $T_C$ , where the ferromagnetic-to-paramagnetic transition takes place. Values of 286 K and 360 K were obtained for  $\text{Pr}_{2/3}\text{Sr}_{1/3}\text{MnO}_3$  and  $\text{La}_{2/3}\text{Sr}_{1/3}\text{MnO}_3$  respectively, in good agreement with the literature [24].

In order to study the transport phenomena, resistivity measurements were not used.

Sample	$\text{Pr}_{2/3}\text{Sr}_{1/3}\text{MnO}_3$ Pbnm-(O')	$\text{La}_{2/3}(\text{Sr})_{1/3}\text{MnO}_3$ R-3c
Lattice parameters		
a	5.4570(2)	5.5017(1)
b	5.4896(1)	
c	7.7044(2)	13.3609(1)
Bond length and angles		
$d_{\text{Mn-O(I)}}$	1.957(2)	1.9510(2)
$d_{\text{Mn-O(II)}}$	2.00(1)	1.9510(2)
$d_{\text{Mn-O(III)}}$	1.90(1)	1.9510(2)
$\theta_{\text{Mn-O(I)-Mn}}$	159.3(1)	167.60(1)
$\theta_{\text{Mn-O(II)-Mn}}$	163.8(5)	167.60(1)
$\langle r_{\text{A.Ln}} \rangle$	1.222	1.247
tolerance factor	0.924	0.933
Goodness of Fit	1.47	1.91
Rb	5.77	5.23

Table 1. Room temperature structural parameters refined for both phases. The site occupancies were kept at fixed values consistent with the nominal stoichiometry. For Pbnm, the atomic positions are:  $\text{Pr}^{3+}/\text{Sr}^{2+}$ : 4c (x, y, 0.25);  $\text{Mn}^{3+}/\text{Mn}^{4+}$ : 4a (0, 0, 0);  $\text{O}^{2-}(\text{I})$ : 4c (x, y, 0.25);  $\text{O}^{2-}(\text{II})$ : 8d (x, y, z). The hexagonal axes setting were used for the refinement of the structure belonging to the R-3c space group. The atomic positions are:  $\text{La}^{3+}/\text{Sr}^{2+}$ : 6a (x, y, 0.25);  $\text{Mn}^{3+}/\text{Mn}^{4+}$ : 6b (0, 0, 0);  $\text{O}^{2-}$ : 18e (x, 0, 0.25). Numbers in parenthesis are standard deviations. (J. Mira et al. [45]).

Seebeck effect measurements were preferred as measuring technique, because the Seebeck coefficient,  $\alpha(T)$ , depends only on temperature and potential gradients between two measuring points [47]. This eliminates the dependence of the data on sample shapes. Also, Palstra et al. [48] have signaled that thermopower provides unique insight into the transport mechanisms of these materials. Measurements of  $\alpha(T)$  were performed with a homemade apparatus similar to the described by Goodenough et al. [49]. A temperature difference of 1 K was applied between two parallel cuts of the sample. The sign of the temperature difference was reversed in order to check the results. The

cuts were done so that they were perpendicular to the c-axis, and other two perpendicular to the ab-plane. Only slight deviations from the desired orientation of less than 0.5 degrees in PrSr and 4 degrees in LaSr were observed.

First,  $\alpha(T)$  was measured along the c-axis and parallel to the ab-plane in  $\text{Pr}_{2/3}\text{Sr}_{1/3}\text{MnO}_3$ . The results are presented in Fig. 6(a). It is seen that the coefficient is the same in both directions below  $T_C$ . In the ferromagnetic phase the value is very small, as in similar materials [48]. At a temperature similar to the  $T_C$  estimated from dc-magnetization measurements, a jump is observed, as expected; but an important difference is detected:  $\alpha(T)$  along the ab-plane is around a 15 % higher (in absolute value) than along the c-axis. This result is basically similar to the one of Zeng and Wong [44], who report anisotropy of the transport properties for temperatures above the region where the ferromagnetic-to-paramagnetic phase transition of their LaCaMnO thin films takes place. The situation is different for  $\text{La}_{2/3}\text{Sr}_{1/3}\text{MnO}_3$  (Fig. 6(b)): below  $T_C$  the behavior is similar to the previous case,  $\alpha(T)$  is equal for both the c-axis and the ab-plane; nevertheless, for  $T > T_C$  the conducting regime keeps on being isotropic.

In order to analyze the results, the crystal structure of both materials must be taken into account. Both present a distorted perovskite structure, but the spatial groups are different.  $\text{Pr}_{2/3}\text{Sr}_{1/3}\text{MnO}_3$  crystallizes in the orthorhombic Pbnm structure and  $\text{La}_{2/3}\text{Sr}_{1/3}\text{MnO}_3$  in the rhombohedral R-3c one. The key is that for the Pbnm case the Mn-O-Mn bond lengths and angles are different. In the case of the R-3c structure all the Mn-O-Mn bonds and angles are equivalent (see Table 1). Provided that the transfer integral between two Mn sites (and therefore the conductivity of such bond) is strongly dependent on the bond angle [50], the conclusion is that the origin of the anisotropic

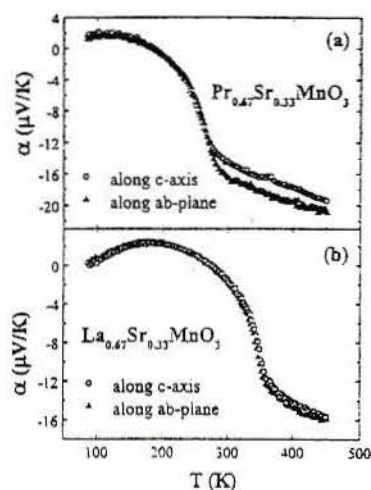


Figure 6. (a) Temperature dependence of the thermoelectric power of a  $\text{Pr}_{0.67}\text{Sr}_{0.33}\text{MnO}_3$  single crystal, along the c-axis and along the ab-plane. Note the difference in  $\alpha(T)$  for  $T > T_C$  depending on the orientation of the crystal. (b) The same for a  $\text{La}_{0.67}\text{Sr}_{0.33}\text{MnO}_3$  single crystal. The behavior is now isotropic in all the studied temperature range. (J. Mira et al. [45]).

behavior in the transport properties lies in the different crystal structures. The crossover from orthorhombic to rhombohedral symmetry in  $\text{L}_{2/3}\text{A}_{1/3}\text{MnO}_3$  perovskites takes place at a geometric tolerance factor (defined as  $t = d((L,A)-O) / \sqrt{2} d(\text{Mn}-O)$ , where  $d((L,A)-O)$  and  $d(\text{Mn}-O)$  are mean equilibrium bond lengths) value of about 0.93 [51]. For the compounds considered here  $\text{Pr}_{2/3}\text{Sr}_{1/3}\text{MnO}_3$  has  $t = 0.924$  and  $\text{La}_{2/3}\text{Sr}_{1/3}\text{MnO}_3$   $t = 0.933$ , i.e. one at each side of the boundary line at  $t \approx 0.93$  [52].

In our opinion, the physical implications of such crossover have not been conveniently highlighted. In a recent investigation of the ferromagnetic-to-paramagnetic phase transition in  $\text{La}_{2/3}(\text{Ca},\text{Sr})_{1/3}\text{MnO}_3$  perovskites, it was

found that an increase of the Sr-doping (and therefore of the tolerance factor) leads to a qualitative change of the nature of the magnetic phase transition, which goes from first- to second order type [31]. The change takes place at  $t \approx 0.93$ . Such coincidence with the aforementioned boundary line makes us to think that there might be a relationship between the crystal structure and the physics governing the behavior of these materials [53]. As orthorhombic symmetry allows a cooperative Jahn-Teller (JT) distortion and the rhombohedral one does not [54], effects like the qualitative changes of the type of phase transition might be consequences of the disappearance of the cooperative JT distortion (pointed out to be important in the physics of these perovskites [16]).

Consequently, we think that a phase diagram, separating anisotropic from isotropic conduction regimes, can be set for all the  $\text{L}_{2/3}\text{A}_{1/3}\text{MnO}_3$  perovskites, with a phase boundary at  $t \approx 0.93$ , which is also the boundary of the orthorhombic-to-rhombohedral phases [45].

#### 4. MAGNETIC PHASE TRANSITION IN COBALT PEROVSKITES

The substitution of Mn by Co in the perovskite adds another dimension of complexity due to the changing nature of the spin state of  $\text{Co}^{3+}$  ions [55-65]. At low temperatures the Co is in low spin state ( $t_{2g}^6 e_g^0 \Rightarrow S=0$ ), but the energetic proximity of this configuration with intermediate spin ( $t_{2g}^5 e_g^1 \Rightarrow S=1$ ) or high-spin ( $t_{2g}^4 e_g^2 \Rightarrow S=2$ ) configurations, of the order of 0.02 eV, makes possible a thermal activated excitation from  $S=0$  to  $S=1$  or  $S=2$  states at moderate temperatures when  $L = \text{La}$  [55-65]. With other rare-earths than La the spin transition takes place at higher temperatures [66].

The system  $\text{La}_{1-x}\text{Sr}_x\text{CoO}_3$  does not show

CMR [67-69], unlike manganites, but it has a similar magnetic behaviour, with ferromagnetic interactions setting up with increasing  $x$  [3,59,70,71]. However, the thermally and compositionally induced spin state changes in the Co ions add some peculiarities to this system. The non-homogeneity of the spin state of these ions might affect the cooperative behaviour of the Co sublattice, and concretely, the FM-PM phase transition. This idea, together with the lack of a proper study of such transition led us to the determination of its critical exponents, in the search for differences of this system with the manganites [72].

$\text{La}_{1-x}\text{Sr}_x\text{CoO}_3$  samples with  $x=0.20, 0.25$  and  $0.30$  were prepared by conventional ceramic methods [72]. X-Ray powder diffraction revealed that all the samples are single phase. The temperature dependence of resistivity was checked with a standard four probe technique. Magnetic data were taken by VSM magnetometry between 77 and 300 K up to 15 kOe maximum applied magnetic fields.

Zero field cooled (ZFC) and field cooled (FC) dc magnetization under magnetic fields of 1 kOe and 20 Oe were measured. Figure 7(a) shows ZFC data for  $H=20$  Oe. For  $x=0.25$  and  $0.30$  the increment in magnetization around  $T=240$  K (considered so far as the Curie temperature of the FM-PM phase transition) marks the onset of ferromagnetic interactions. For  $x=0.20$  this onset takes place at lower temperature. These results are basically in agreement with previous literature, excepting the fact that in [71] a lower onset temperature for  $x=0.20$  is given. In this study, particular attention to the behaviour near the FM-PM phase transition was paid. A first rough evaluation of the transition temperature was done through the determination of the maximum slope of the temperature dependence of the magnetization. Further measurements below and above the so determined ordering temperature were performed. As a general

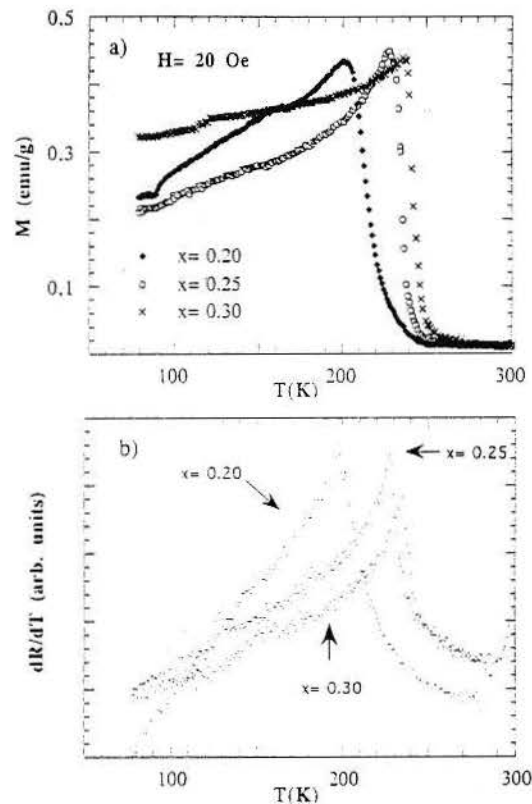


Figure 7. (a) ZFC magnetization vs. temperature under a field of 20 Oe, and (b) derivative of the resistivity vs. temperature curves for  $\text{La}_{1-x}\text{Sr}_x\text{CoO}_3$  ( $x=0.20, 0.25$  and  $0.30$ ) samples (the temperatures at which they display the maxima are taken as  $T_C^*$ ). (J. Mira et al. [72]).

example, Fig. 8 shows the magnetization vs. field isotherms for the particular case  $x=0.30$ . Note that saturation magnetization is not fully reached. The same was found for other studied compositions, in agreement with Itoh et al. [71], who pointed out the absence of true long range order (LRO) ferromagnetism in these compounds. To obtain information on the high-field behaviour near the critical region,

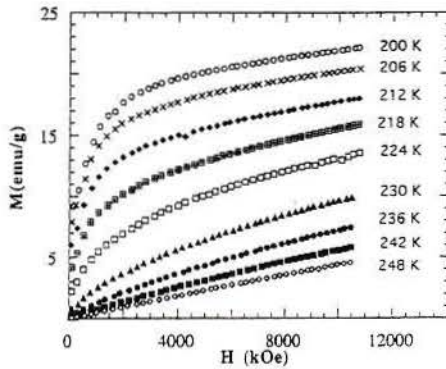


Figure 8.  $M$  vs.  $H$  curves at several temperatures for  $\text{La}_{0.7}\text{Sr}_{0.3}\text{CoO}_3$ . (J. Mira et al. [72]).

magnetization curves were measured using fields as high as 55 kOe [73]. The approach to the magnetic saturated state has been analyzed considering the general empirical relationship:

$$M = M_S(\sum_i (a_i/H^i)) + bH \quad (1)$$

where  $M_S$  is the spontaneous magnetization and  $a_i$  denote the coefficients for the corresponding  $H^i$  terms. The term  $bH$  represents the increase in spontaneous magnetization caused by the increased alignment of spins in the high field regime. As a general comment, we can say that these coefficients take rather high values [73], which indicates a somehow strong difficulty to reach saturation as a consequence of the cluster-glass nature of the sample. The temperature dependence of the  $a_i$  coefficient exhibits a clear increase below  $T_C$ . Measurable values are obtained in the interval of temperatures just above the evaluated order temperature [73], indicating that some type of magnetic structure is still present. From the isotherms of Fig. 8 the initial susceptibility,  $\chi_0$ , was evaluated. Corrections of the demagnetizing field were taken into account.

First of all, in order to discard the possibility of a first-order phase transition, the criterion

given by Banerjee [32] was used. In the present cases the slope of the isotherm plots of  $H/M$  vs.  $M^2$  is positive, therefore, following Banerjee's criterion we assume that the FM-PM phase transition in these cobaltites is basically of second order. In the region around the phase transition, the following expressions hold for the magnetization and the initial susceptibility,  $\chi_0$ ,

$$\chi_0^{-1}(T) \propto (T-T_C)^{1/\gamma}, \text{ for } T > T_C \quad (2)$$

$$M(H) \propto H^\delta, \text{ for } T = T_C \quad (3)$$

$$M_S(T) \propto (T_C - T)^{1/\beta}, \text{ for } T < T_C \quad (4)$$

In order to properly determine the Curie temperature as well as the critical exponents  $\beta$ ,  $\gamma$  and  $\delta$  for the magnetization and the inverse initial susceptibility respectively, the modified Arrott plots technique was used [74] considering the temperature interval  $\varepsilon = |T_C - T|/T_C < 0.05$ . A self consistent method to obtain the best fitting was considered. Starting from an initial estimation of the values of the critical exponents, modified Arrott plots are constructed. The spontaneous magnetization as a function of the temperature is determined from the intersection of the linear extrapolation of the straight line in the modified Arrott plots with the  $M^{1/\beta}$  axis, while the inverse of the susceptibility corresponds to the intersection of these lines with the  $(H/M)^{1/\gamma}$  axis. These data are fitted to the exponential behavior of Eqs. (2) and (4). New values for the critical exponents are thus obtained, and re-introduced in the scaling of the modified Arrott plot axis. The process is repeated until the iteration converges, leading to the optimum fitting values. Figure 9 shows the behaviour for  $x=0.25$  of  $M^{1/\beta}$  and  $(H/M)^{1/\gamma}$  for the  $\beta$  and  $\gamma$  values corresponding to the optimum fitting.  $\delta$  is calculated from the Widom scaling relation  $\delta = 1 + \gamma/\beta$ . Direct fits of  $\delta$  taking into account that near  $T_C$   $M \approx H^\delta$  give values close to the obtained from the scaling relation ( $\delta = 3.96$  and  $4.07$  for  $x=0.20$  and  $x=0.30$  respectively). The

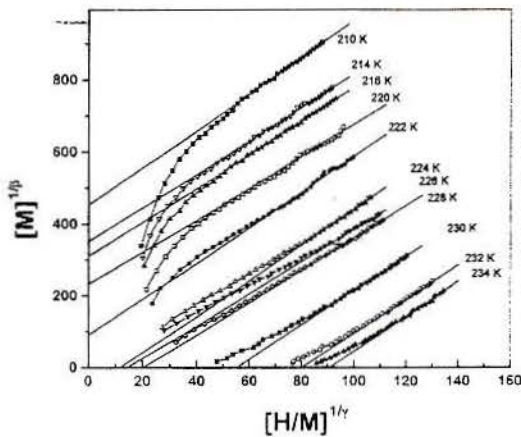


Figure 9. Modified Arrott plot isotherms on  $\text{La}_{0.75}\text{Sr}_{0.25}\text{CoO}_3$  for the optimum fitting ( $\beta = 0.46$ ,  $g = 1.39$ ). (J. Mira et al. [72]).

data for the critical temperature,  $T_C$  and the critical exponents are collected in Table 2. It must be emphasized that a quite careful study has to be done in order to achieve properly the critical exponents and  $T_C$ . Special care must be paid to the search for optimum fittings. The roughness of many of the fits found in the literature for the manganites explains the important differences found from author to author for the critical exponents in similar systems. Also, to fully describe the behaviour at the phase transition not only the ferromagnetic phase, but also the paramagnetic one must be analyzed, in order to calculate a complete set of critical exponents.

The temperature dependence of resistivity was also checked. The results, shown in Fig. 7(b), are in agreement with previous reports [68,69]. The samples are metallic and a decrease in temperature within the ferromagnetic region affects only the thermal dependence of the metallic behaviour under a temperature  $T_C^*$ , due to magnon scattering [75], but not the metallic regime, that continues above  $T_C^*$ . The values of  $T_C^*$  are shown in Table 2. From

this table, the first remarkable result is the discrepancy between the values of the transition temperatures and the temperatures of change of the thermal dependence of resistivity,  $T_C^*$  for samples  $x=0.25$  and  $0.30$ . Provided that magnon dispersion is responsible for the change in the resistivity evolution, bulk ferromagnetism should be necessary for the variation of slope in resistivity, therefore we expected  $T_C^*$  to be equal to  $T_C$ , and in fact in the past it has been interpreted so. This means that authors willing to study critical phenomena through observations of the electrical conductivity should proceed with caution and know of the absence of a critical point at  $T_C^*$ . In order to gain insight into this the temperature dependence of coercivity was measured [73]. Non-negligible values of the coercive fields were observed above the Curie point determined by the critical exponents analysis. Also, the correlation between temperature dependence of coercivity,  $H_C$ , and that of spontaneous magnetization,  $M_S$ , as derived from the modified Arrott plots, has been checked considering

$$H_C(T) \propto M_S(T)^n \quad (5).$$

A value of  $n \approx 4.1$  is found [73], which in principle is associated to a relatively five-fold basal magnetic anisotropy (as  $H_C \approx K/M_S$ , being  $K$  the anisotropy constant), that should be correlated to the structure nature of the

$x$	$T_C$ (K)	$T_C^*$ (K)	$\beta$	$\gamma$	$\delta$
0.20	198.5	198	0.46	1.39	4.02
0.25	222.3	228	0.46	1.39	4.02
0.30	223.4	235	0.43	1.43	4.38

Table 2. Transition temperatures obtained from modified Arrott plots ( $T_C$ ), peak temperature of the temperature derivative of resistance ( $T_C^*$ ), and critical exponents of the magnetic phase transition for  $\text{La}_{1-x}\text{Sr}_x\text{CoO}_3$  compounds with  $x = 0.20, 0.25, 0.30$ . (J. Mira et al. [72]).

perovskite. This five-fold anisotropy might be due to a intermediate-spin state of the Co ions. Ibarra et al [76], have found a huge anisotropic magnetostriction in similar samples and attributed it to a field-induced instability of the Co ions. Links between the results of Ibarra et al. and the five-fold anisotropy reported by some of us in [73] should deserve attention. An anomalous magnetic character has been found in the region around the Curie temperature, in particular for the sample with  $x=0.30$ . It is firstly remarkable that there is a difference in the value of the order temperature when magnetic measurements are analyzed by different methods (kink point and Arrott plots). In fact, a deviation of more than 20 K is observed. The peculiar character is also deduced from the non-vanishing values of the coercivity and the coefficients of the law of approach to saturation [73]. Reports on this series also support this anomalous behaviour around the Curie temperature. Magnetostriction takes vanishing values not before 250 K [76], while neutron scattering and small angle scattering experiments reveal the existence of regions of short-range order above  $T_C$  [77,78].

In order to make an interpretation of the critical exponents, after Fisher et al. [79], from a renormalization group analysis of systems with exchange interaction of the form  $J(r)=1/r^{d+\sigma}$  ( $d$ = dimension of the system,  $\sigma$  = range of the interaction), mean field critical exponents correspond to LRO ( $\sigma > 2$ ). Theoretical predictions give  $\beta = 0.5$ ,  $\gamma = 1$ ,  $\delta=3$  for such a case. This is found by Mohan et al. in  $\text{La}_{0.8}\text{Sr}_{0.2}\text{MnO}_3$  [40], who report  $\beta = 0.5$ ,  $\gamma = 1.08$ ,  $\delta=3.13$ . It is plausible if the metallicity induced in these materials by ferromagnetic interactions is considered. Also, Lofland et al.[39] use  $\beta = 0.5$ ,  $\gamma= 1$  to fit the Curie point with Arrott plots in the same compound. It must be noted that in the manganites, for slightly higher doping ranges ( $x > 0.25$ ) some authors [24,80] have signaled the incompatibilities of a smooth second-order

transition with their results and have pointed out the existence of a first-order transition attending to thermal irreversibilities in the resistance, abrupt variations in the double exchange coupling energy [24] and a discontinuous change in the mean kinetic energy of the Mn 3d electrons [28]. In recent neutron diffraction studies [77,78] an anomalous change of the Co-O bond length has been observed in  $\text{La}_{0.7}\text{Sr}_{0.3}\text{CoO}_3$  above  $\approx 220$  K (at a value similar to the one extracted for  $T_C$  from our fits), associated to a transition from itinerant to polaronic regime. It might be an argument to suspect about a first-order transition, but, in any case we have concluded before that this transition is of second order.

In principle, mean field exponents, like in the manganites, should be expected in the FM-PM transition in  $\text{La}_{1-x}\text{Sr}_x\text{CoO}_3$ , but our results (Table 2) give a  $\beta$  coefficient not so high as expected (0.5). Even more, the  $\gamma$  value is very close to that corresponding to a Heisenberg model. In the only report to our knowledge on a related compound, Menyuk et al. [81] studied the critical exponents of the FM-PM phase transition of  $\text{La}_{0.5}\text{Sr}_{0.5}\text{CoO}_3$ . For this doping degree the material does not present a distortion of the perovskite cubic structure [82] and they expected  $\gamma = 1.4$ , applying the high temperature thermal expansion calculation of the classical Heisenberg model with nearest neighbour interactions [83]. They got 1.27, and tried to justify the deviation invoking the role of more-distant neighbour interactions. Difficulties in the achievement of the correct phase might also be involved. In fact, Señaris-Rodríguez and Goodenough [59] have recently noted the difficulty to achieve full oxygen stoichiometry in  $\text{La}_{1-x}\text{Sr}_x\text{CoO}_3$  for  $x \geq 0.30$ .

According to our results  $\gamma$  corresponds to a Heisenberg model but  $\beta$  is more mean-field-like, what distorts a global composition. As  $\beta$  is calculated from fittings below  $T_C$  (Eq. 4) and  $\gamma$  above that point (Eq. 2) there could be a room for other changes not considered till

now. One of them might be changes in the spin state of the  $\text{Co}^{3+}$  ions due to the alterations of the Co-O bond length. In fact several authors [84,85] have already stressed the strong influence of such a bond length on the electronic state of  $\text{LaCoO}_3$ . As we have already mentioned, the abrupt increase in the Co-O bond length for the  $x=0.30$  sample at  $T_C$  could cause a spin-state transition simultaneously with the FM-PM transition. This picture would indicate that different regimes are fitted above and below  $T_C$ . Ibarra et al. [76] have found a huge anisotropic magnetostriction in  $\text{La}_{1-x}\text{Sr}_x\text{CoO}_3$ , and attributed it to a field-induced orbital instability, more concretely to a transition from a nondegenerated low-spin state of the  $\text{Co}^{3+}$  ions to an orbital degenerated intermediate spin-state (IS), which is a Jahn-Teller ion. Under Jahn-Teller distortion [JT], the doubly degenerated  $e_g$  level of IS- $\text{Co}^{3+}$  splits into two singlets ( $L=0$ ), and the triplet  $t_{2g}$  into a singlet and a doublet ( $L=1$ ). The singlet states of the  $t_{2g}$  level are occupied by two electrons with opposite spins and the doublet level by three electrons. Due to the degeneracy of the doublet level with nonzero angular momentum, a strong intra-atomic spin-orbit coupling is created which couples to the lattice strain to give rise to a large anisotropic magnetostriction [76]. The five-fold character of the anisotropy, estimated from fits of coercive fields vs. spontaneous magnetization [73], might be an evidence of such intermediate spin state.

At this point one concern must be addressed. Why do  $\text{La}_{1-x}\text{Sr}_x\text{CoO}_3$  ( $x \geq 0.20$ ) behave so different compared to the doped manganites? Or equivalently, why do the studied materials behave so close to a Heisenberg model, provided that it does not apply properly to metallic conductors like these? The ground reason is to be searched in the changing nature of the  $\text{Co}^{3+}$  spin state, which makes the difference with the unaltered  $\text{Mn}^{3+}$  spin state

in the manganites (as it has been remarked in several papers [59,69,86], and specially by Gayathri et al. [87] in a study of  $\text{La}_{0.7}\text{Ca}_{0.3}\text{Mn}_{1-x}\text{Co}_x\text{O}_3$  mixed compounds), and in the phase segregation taking place in these cobaltites [59]. After Señaris-Rodríguez and Goodenough [59] the Sr content leads to hole-rich metallic ferromagnetic regions and a hole-poor matrix similar to  $\text{LaCoO}_3$ . These regions are isolated until  $x=0.20$ , where the ferromagnetic clusters reach a percolation threshold and order ferromagnetically below  $T_C$ . But despite of the percolation, the hole-poor matrix still persists and within it the  $\text{Co}^{3+}$  spin state is in a ratio 50:50 high-spin/low-spin. Here the hole-poor portions of the material with diamagnetic  $S=0$  ions will act diluting the magnetic lattice and preventing a global LRO. It could also be the reason for the high  $\beta$  in the framework of a Heisenberg model. Poon and Durand [88] studied in the seventies the critical behaviour of amorphous ferromagnets. They detected a trend of enhanced values of  $\beta$  in amorphous alloys that contained at least one nonmagnetic component, and explained it in terms of a dilution model. They supported their results on simulations done by Müller-Krumbhaar [89] on homogeneous Heisenberg spin systems with missed spin clusters. In these simulations it was found that the local value of  $\beta$  increased close to the missed clusters (increasing therefore the the bulk value as well). In our case, the hole-poor regions might be acting equivalently to missed spins. The discrepancies between the Curie temperature and the temperature of change of slope in resistivity are similar to those reported by Lofland et al. [39] in  $\text{La}_{0.8}\text{Sr}_{0.2}\text{MnO}_3$ , and our reasoning will be in some aspects similar:  $T_C$  marks only the break of cluster ordering, but the clusters can persist above  $T_C$ , and short range magnetic correlations could take place between them. If the lifetime of such magnetic correlations is larger than the transport time, from an electronic point of view the carriers see a global ferromagnetic-

like environment. These different time scales underlie the coexistence of a magnon dispersion without having global ferromagnetism from a static measurement point of view. From  $x=0.25$  to  $x=0.30$ ,  $T_C$  remains almost the same, but  $T_C^*$  increases from 227 to 235 K, indicating that the clusters have grown and enable a FM environment to the carriers up to higher temperatures. On the other hand, the growth does not affect the ordering among clusters, so  $T_C$  is not altered. Another interpretation might be that the magnetic transition from non-homogeneous cluster-glass ferromagnetism [90] to paramagnetic behaviour takes place seemingly, not in a sharp conventional way, since the temperature interval for the transition is rather extended.

In summary, through an analysis of the critical exponents at the second order FM-PM phase transition on the title compounds we have obtained that the system is better described with a Heisenberg model than with a mean field one, suitable for manganese perovskites. This means also the absence of long-range interactions due probably to the presence of segregated  $\text{LaCoO}_3$ -like hole-poor regions that would hinder them. Also, the  $\beta$  value is larger than expected for a Heisenberg model, which could be understood if a spin-state transition takes place at  $T_C$  (yielding different magnetic species above and below  $T_C$ ) or if such hole-poor regions act equivalently to missed spin clusters in amorphous ferromagnets.

##### **5. CONDUCTIVITY OF $\text{La}_{1-x}\text{Sr}_x\text{CoO}_3$ FERROMAGNETIC PEROVSKITES THROUGH THE MAGNETIC PHASE TRANSITION: TRANSITION FROM ITINERANT TO POLARONIC.**

From a conducting point of view, the  $\text{La}_{1-x}\text{Sr}_x\text{CoO}_3$  system exhibits a metallic phase for  $x \geq 0.20$ , which persists even above  $T_C$  [59].

The substitution of Sr for La introduces  $x$  holes per formula unit into the  $\text{CoO}_3$  array. The holes stabilize IS clusters containing  $\sigma^*$  electrons introducing ferromagnetic interactions between the localized spins of the  $t^5$  configurations within clusters which have metallic conductivity [59]. Señarís Rodríguez and Goodenough have determined by Seebeck measurements a transition temperature,  $T_S$  ( $T_S \approx 300$  for  $x=0.30$ ), and interpreted it as the maximum temperature for a dynamic ordering of HS and LS ions [59]. Caciuffo et al. [77,78], by means of neutron diffraction experiments in  $\text{La}_{0.7}\text{Sr}_{0.3}\text{CoO}_3$ , have observed a transition at  $T_C$  from itinerant  $\sigma^*$  electrons in a percolating IS state to a dynamic phase segregation producing the appearance of clusters of a ferromagnetic second phase with a Curie temperature  $T_C^* \approx 300 \text{ K} > T_C$ . An anomalous increase in the thermal expansion signals the introduction of localized IS and/or HS configurations and accompanies the segregation into hole-rich clusters from a hole-poor matrix [77,78]. The temperature dependence of the rhombohedral cell parameter was found to be anomalous at the Curie temperature, exhibiting a high deviation from a Grüneisen approximation, as seen in Figure 10. The Co-O bond lengths remain constant on warming up to  $T_C$  but increase steadily in the paramagnetic phase, as can be seen in Figure 11. The correlation between the temperature variation of the Co-O bond length and the anomalous thermal expansion of the lattice, can be assumed just by inspecting the inset of Figure 11. A similar anomaly in the thermal expansion has been observed for  $\text{La}_{2/3}\text{Ca}_{1/3}\text{MnO}_3$  and interpreted as the effect of a gradual carrier localization process with the formation of magnetic polarons [22]. This conclusion was supported by magnetic small-angle neutron scattering (SANS), which grew in intensity on warming at the boundary between the ordered and disordered magnetic phases. A similar experiment was made in  $\text{La}_{0.7}\text{Sr}_{0.3}\text{CoO}_3$  to verify whether a similar

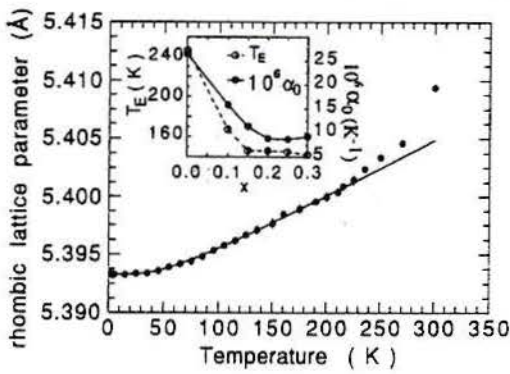


Figure 10. Temperature dependence of the rhombohedral lattice parameter for  $\text{La}_{0.7}\text{Sr}_{0.3}\text{CoO}_3$ . The solid line is a fit to the Grüneisen-Einstein model with the parameters quoted by Caciuffo et al. [78]. The  $x$ -dependence of the Einstein temperature  $T_E$  and the linear thermal expansion coefficient,  $\alpha_0$ , for  $T \gg T_E$  is shown in the inset. (Caciuffo et al. [77,78]).

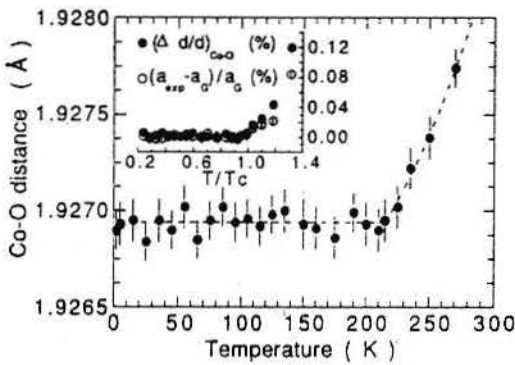


Figure 11. The equilibrium bond length  $d$  as a function of temperature for  $\text{La}_{0.7}\text{Sr}_{0.3}\text{CoO}_3$ . The broken line is a guide to the eye. The inset shows the comparison between the relative variation  $[d(T) - d(0)]/d(0)$  and the relative departure of the lattice parameter from the value predicted by the Grüneisen-Einstein formula. (Caciuffo et al. [77,78]).

phenomenology occurs. It was found that, on warming through  $T_C$ , the number of magnetic inhomogeneities suddenly increases as does their size (Figure 12). The fact that the magnetic susceptibility presents a strong deviation from the Curie-Weiss law, which persists well above  $T_C$  (Figure 13), together with the fact that in a SANS experiment the energy of the scattering beam is not analyzed and what is obtained is the response integrated over a large energy window centered at zero energy transfer, indicates that the system enters into a cluster-fluctuation regime below  $T \approx 300$  K. The zero-temperature ordered magnetic moment is of  $1.7 \mu_B/\text{Co}$ . In the framework of the phase diagram of Señarís Rodríguez and Goodenough [59] this suggests the presence below  $T_C$  of a majority phase with Co ions in the IS configuration  $t^5\sigma^{*1-x}$ , and any LS Co (III)-rich minority phase occupies a relatively small volume. With localized electrons in the  $t$  states and itinerant electrons in a  $\sigma^*$  band of  $e$ -orbital parentage, the most straightforward interpretation of these

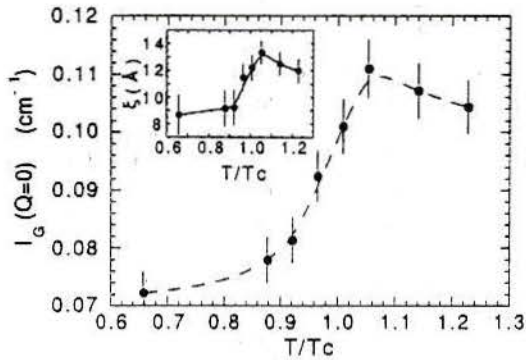


Figure 12. Intensity at  $Q = 0$  of the temperature dependent SANS Guinier component from  $\text{La}_{0.7}\text{Sr}_{0.3}\text{CoO}_3$ . The Guinier term is attributed to the presence of ferromagnetic clusters with spatial extension  $\xi$  (inset). The lines are guides to the eye. (Caciuffo et al. [77]).

experimental results is a segregation above  $T_C$  of a hole-rich superparamagnetic volume fraction into a hole-poor paramagnetic region. Retention of a metallic temperature dependence of the conductivity above  $T_C$  requires that the superparamagnetic clusters remain mobile like large magnetic polarons having a mobility that is not activated, but is nevertheless constrained by strong coupling to cooperative oxygen-atom vibrations. A relatively large coherence length for the paramagnetic domains, up to 15 Å, suggests that each contains more than one mobile hole, which would mean they are not conventional magnetic polarons but are more easily understood as second-phase vibronic domains at a cross-over from localized to itinerant behaviour of the  $\sigma^*$  electrons. Such a phase segregation can also account for the sudden onset of an increase of the Co-O bond length on heating above  $T_C$ . A AMO3 perovskite that would retain  $(180 - \phi)$  M-O-M bonding via  $\sigma^*$  electrons in a narrow band of width  $W_\sigma \sim \cos \phi \langle \cos(\theta_{ij}/2) \rangle$ , where  $\theta_{ij}$  is the angle between localized spins on neighboring M atoms, has a thermal expansion that occurs preferentially in the A-O bond length. In  $\text{La}_{0.7}\text{Sr}_{0.3}\text{CoO}_3$ , thermal expansion of the A-O bonds with retention of a constant Co-O bond length increases towards unity the geometric tolerance factor,  $t = d(\text{La-O})/\sqrt{2}d(\text{Co-O}) < 1$ . Increasing  $t$  decreases  $\phi$  and broadens  $W_\sigma$  in opposition to its narrowing by increased spin-disorder scattering. At  $T_C$ , the bending angle  $\phi$  has become small, and the loss of long-range magnetic order narrows  $W_\sigma$  sufficiently that the system breaks up into isolated superparamagnetic clusters in a paramagnetic matrix. The superparamagnetic clusters are clearly manifest in the interval  $T_C < T \leq 300$  K not only by the SANS data, but also by the deviation of the paramagnetic susceptibility from a Curie-Weiss law (Figure 13). Magnetic ordering within the superparamagnetic clusters occurs below  $T^* \approx 300$  K, which indicates they are not conventional magnetic polarons; some new

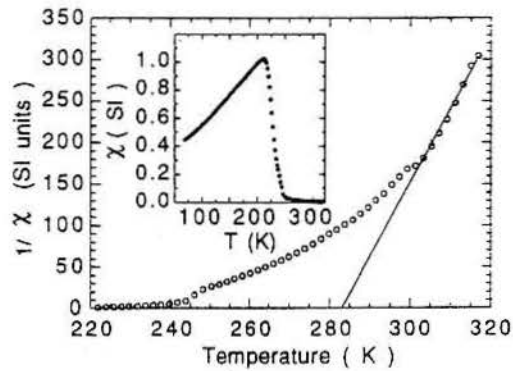


Figure 13. Temperature dependence of the inverse magnetic susceptibility  $1/\chi$  for  $\text{La}_{0.7}\text{Sr}_{0.3}\text{CoO}_3$ . The solid line is a fit to a Curie-Weiss law. (Caciuffo et al. [77,78]).

spin configuration is being stabilized in the superparamagnetic clusters. The abrupt increase in the thermal expansion of  $d(\text{Co-O})$  above  $T_C$  indicates electron localization and/or the thermal excitation of high-spin  $\text{Co}^{3+}$  configurations above  $T_C$ .  $T^* \approx T_S$ , invites the suggestion that the "magnetic polarons" are, in this case, fluctuations of ordered localized-spin  $e^1$  or  $e^2$  configurations and low-spin  $\text{Co}^{4+}$  nearest neighbors.

The neutron experiments of Caciuffo et al. [77,78] reveal that the increasing cell volume with increasing Sr doping places the  $\sigma^*$  band of the intermediate spin state for  $x=0.3$  at the threshold of a transition from itinerant to localized configurations at  $T_C$ . The Co-O bond length shows little thermal expansion in the ferromagnetic phase in order to retain itinerant-electron behaviour; above  $T_C$  the system transforms to a polaronic state and the mean equilibrium Co-O distance increases. The volume of the magnetic clusters increases with the correlation length of the short-range order, so it decreases with increasing temperature above  $T_C$ ; but at a given temperature it should increase in an applied magnetic field. Where

the paramagnetic matrix contains isolated ferromagnetic clusters above  $T_C$  at  $x \leq 0.20$ , a growth in volume of the hole-rich clusters to a percolation threshold may be the origin of the observed magnetoresistance.

## 6. CONCLUSIONS

The study of phase transitions is of great interest in physics, and therefore in a hot topic like magnetoresistive (MR) perovskites it can provide insight into the fascinating mechanisms governing these materials. Even more if the most appealing phenomena (specially magnetoresistance) take place at the ferromagnetic phase transition. In this review it has become clear that, despite in a first moment it seemed that all the MR perovskites behave similarly, they do not. The key point of the study is the inspection of the dramatic changes happening at the Curie temperature of the ferromagnetic-to-paramagnetic transition, which determines qualitative differences, leading at least to a classification into two groups. The factor causing the differences might be related with the origin of the colossal magnetoresistance. Whenever a final theory of CMR systems is presented, it should explain the behaviour of the materials at their critical point.

## ACKNOWLEDGEMENTS

This article is a review of the work done in collaboration with several groups, composed by A. Fondado, L. E. Hueso, F. Rivadulla, C. Vázquez Vázquez and M. A. López Quintela (Universidade de Santiago de Compostela, Spain), M. P. Breijo and M. A. Señaris Rodríguez (Universidade de A Coruña, Spain), R. Caciuffo, D. Rinaldi, G. Barucca (Università di Ancona, Italy), P. G. Radaelli (Rutherford Appleton Laboratory, UK), D. Fiorani (ICMAT-CNR, Rome, Italy), J. B. Goodenough (University of Texas at Austin, USA), J. M.

García-Beneytez, M. Vázquez, J. Arcas and F. J. Castaño (CSIC / IMA - Universidad Complutense, Spain), A. M. Balbashov (Moscow State Steel and Alloys Institute, Russia) and R. D. Sánchez (Centro Atómico Bariloche - Instituto Balseiro, Argentina). The authors wish to express their gratitude to all these people, which has generated so fruitful collaborations.

The authors wish also thank the DGICYT of Spain for its support under project MAT98-0416.

## REFERENCES

1. Jonker, G., and van Santen, J. 1950, *Physica* 16, 337.
2. Wollan, E., and Koehler, W. 1955, *Phys. Rev.* 100, 545.
3. J. B. Goodenough, J. H. 1955, *Phys. Rev.* 100, 564.
4. Zener, C. 1951, *Phys. Rev.* 81, 403.
5. Anderson, P. W., and Hasegawa, H. 1955, *Phys. Rev.* 100, 675.
6. de Gennes, P. G. 1960, *Phys. Rev.* 118, 141.
7. von Helmolt, R., Wecker, J., Holzapfel, B., Schultz, L., and Samwer, K. 1993, *Phys. Rev. Lett.* 71, 2331.
8. Chahara, K., Ohno, T., Kasai, M., and Kozono, Y. 1993, *Appl. Phys. Lett.* 64, 1990.
9. Jin, S., Tiefel, T. H., McCormack, M., Fastnacht, R. R., Ramesh, R., and Chen, L. H. 1994, *Science* 264, 413.
10. Searle, C. W., and Wang, S. T. 1969, *Can J. Phys.* 47, 2703.
11. Morrish, A. H., Evans, B. J., Eaton, J. A.,

- and Leung, L. K. 1969, *Can. J. Phys.* 47, 2691.
12. Baibich, M. N., Broto, J. M., Fert, A., Nguyen van Dau, F., Petroff, F., Etienne, P., Creuzet, G., Friederich, A., and Chazelas, J. 1988, *Phys. Rev. Lett.* 61, 2472.
13. Bednorz, J. G., and Müller, K. A. 1986. *Z. Physik B* 64, 189.
14. Núñez Regueiro, S. E., and Kadin, A. M. 1996, *Appl. Phys. Lett.* 68, 2747.
15. Furukawa, N. 1994, *J. Phys. Soc. Jpn.* 63, 3214.
16. Millis, A. J., Littlewood, P. B., and Shraiman, B. I. 1995, *Phys. Rev. Lett.* 74, 5144.
17. Millis, A. J., Shraiman, B. I., and Müller, R. 1996, *Phys. Rev. Lett.* 77, 175.
18. Millis, A. J. 1998, *Nature* 392, 147.
19. Guo-Meng, Z., Conder, K., Keller, H., and Müller, K. A. 1996, *Nature* 381, 676.
20. Shengelaya, A. Guo-Meng, Z., Keller, H., and Müller, K. A. 1996, *Phys. Rev. Lett.* 77, 5296.
21. Zhou, J.-S., and Goodenough, J. B. 1998, *Phys. Rev. Lett.* 80, 2665.
22. de Teresa, J. M., Ibarra, M. R., Algarabel, P. A., Ritter, C., Marquina, C., Blasco, J., García, J., del Moral, A., and Arnold, Z. 1997, *Nature (London)* 386, 256.
23. Schiffer, P., Ramírez, A. P., Bao, W., and Cheong, S.-W. 1995, *Phys. Rev. Lett.* 75, 3336.
24. Hwang, H. Y., Cheong, S.-W., Radaelli, P. G., Marezio, M., and Batlogg, B. 1995, *Phys. Rev. Lett.* 75, 914.
25. Urushibara, A., Moritomo, Y., Arima, T., Asamitsu, A., Kido, G. and Tokura, Y. 1995, *Phys. Rev. B* 51, 14103.
26. Ibarra, M. R., Algarabel, P. A., Marquina, C., Blasco, J., and García, J. 1995, *Phys. Rev. Lett.* 75, 3541.
27. Lynn, J. W., Erwin, R. W., Borchers, J. A., Huang, Q., Santoro, A., Peng, J.-L., and Li, Z. Y. 1996, *Phys. Rev. Lett.* 76, 4046.
28. Archibald, W., Zhou, J.-S., and Goodenough, J. B. 1996, *Phys. Rev. B* 53, 14445.
29. Martin, M. C., Shirane, G., Endoh, Y., Hirota, K., Moritomo, Y., and Tokura, Y. 1996, *Phys. Rev. B* 53, 14285.
30. Lofland, S. E., Ray, V., Kim, P. H., Bhagat, S. M., Mannheimer, M. A., and Tyagi, S. D. 1997, *Phys. Rev. B* 55, 2749.
31. Mira, J., Rivas, J., Rivadulla, F., Vázquez Vázquez, C., and López Quintela, M. A. 1999. *Phys. Rev. B* 60, 2998.
32. Banerjee, S. K. 1964, *Phys. Lett.* 12, 16; see also for example Vonsovskii, S. V. 1974, *Magnetism (Vol. 2, Chap. 25)*, Wiley, New York.
33. Landau, L. D. 1937, *Zh. Eksperim. i Teor. Fiz.* 7, 19, 627; Lifshitz, E. M. 1941, *ibid.* 11, 269; Ginzburg, E. M. 1947, *ibid.* 17, 833; Vonsovskii, S. V. 1947, *Izv. Akad. Nauk. SSSR (Ser. Fiz)* 11, 485.
34. Bean, C. P., and Rodbell, D. S. 1962, *Phys. Rev.* 126, 104.
35. Causa, M. T., Tovar, M., Caneiro, A., Prado, F., Ibáñez, G., Ramos, C. A., Butera, A., Alascio, B., Obradors, X., Piñol, S.,

- Rivadulla, F., Vázquez-Vázquez, C., López-Quintela, M. A., Rivas, J., Tokura, Y., and Oseroff, S. B. 1998, *Phys. Rev. B* 58, 3233.
36. Potter, C. D., Swiatek, M., Bader, S. D., Argyriou, D. N., Mitchell, J. F., Miller, D. J., Hinks, D. G., and Jorgensen, J. D. 1998, *Phys. Rev. B* 57, 72.
37. Osborn, R., Rosenkranz, S., Argyriou, D. N., Vasiliu-Doloc, L., Lynn, J. W., Sinha, S. K., Mitchell, J. F., Gray, K. E., and Bader, S. D. 1998, *Phys. Rev. Lett.* 81, 3964.
38.  $M^{1/\beta}$  vs.  $(H/M)^\gamma$  plots, being  $\beta$  and  $\gamma$  the critical exponents of the magnetic phase transition. In references [39] and [40] the authors use or arrive to mean field critical exponents, i. e.,  $\beta=0.5$ ,  $\gamma=1$ ; therefore, in practice they are  $M^2$  vs.  $(H/M)$  plots, which constitutes a Banerjee plot with swapped axes.
39. Lofland, S. E., Bhagat, S. M., Ghosh, K., Greene, R. L., Karabashev, S. G., Shulyatev, D. A., Arsenov, A. A., and Mudovskii, Y. 1997, *Phys. Rev. B* 56, 13705.
40. Mohan, Ch. V., Seeger, M., Kronmüller, H., Murugaraj, P., and Maier, J. 1998, *J. Magn. Magn. Mater.* 183, 348.
41. Rosenkranz, S., Osborn, R., Mitchell, J. F., Vasiliu-Doloc, L., Lynn, J. W., Sinha, S. K., and Argyriou, D. N. 1998, *J. Appl. Phys.* 83, 7348.
42. Ramírez, A. P. 1997, *J. Phys.: Condens. Matter* 9, 8171.
43. Kimura, T., Tomioka, Y., Kuwahara, H., Asamitsu, A., Tamura, M., and Tokura, Y. 1996, *Science* 274, 1698.
44. Zeng, X. T., and Wong, H. K. 1998, *Appl. Phys. Lett.* 72, 740.
45. Mira, J., Fondado, A., Hueso, L. E., Rivas, J., Rivadulla, F., and López-Quintela, M. A. 2000, *Phys. Rev. B* 61, 5857.
46. Balbashov, A. M., Karabashev, S. G., Mukovskiy, Ya. M., and Zverkov, S. A. 1996, *J. Cryst. Growth* 167, 365.
47. Elliott, S. R. 1998, *The physics and chemistry of solids*, John Wiley & Sons, New York.
48. Palstra, T. T. M., Ramírez, A. P., Cheong, S.-W., Zegarski, B. R., Schiffer, P., and Zaanen, J. 1997, *Phys. Rev. B* 56, 5104.
49. Goodenough, J. B., Zhou, J.-S., and Chan, J. 1993, *Phys. Rev. B* 47, 5275.
50. Fontcuberta, J., Martínez, B., Seffar, A., Piñol, S., García-Muñoz, J. L., and Obradors, X. 1996, *Phys. Rev. Lett.* 76, 1122.
51. Radaelli, P. G., Iannone, G., Marezio, M., Hwang, H. Y., Cheong, S.-W., Argirou, J. D., and Argyriou, D. N. 1997, *Phys. Rev. B* 56, 8265.
52. For each composition  $\langle r_A \rangle$  (average ionic radius of the A site) was calculated from the tabulated values of Shannon, R. D. 1976, *Acta Cryst.* A32, 751, for atoms in ninefold coordination. The choice of an effective coordination number of 9 instead of 12 for La, Pr and Sr is justified on the basis of the spontaneous cooperative puckering of the  $MnO_6$  octahedra as a consequence of the small size of these central cations. The room temperature, ambient-pressure tolerance factor was calculated from the sum of the empirical ionic radii given in the above mentioned samples. Different values of  $t$  for same compounds can be found in the literature, due to the different sources taken for ionic radii data.
53. Mira, J., Rivas, J., Hueso, L. E., Rivadulla, F., López-Quintela, M. A., Señarís-Rodríguez,

- M. A., and Ramos, C. A. (unpublished).
54. The JT distortion modes are tetragonal or orthorhombic, rhombohedral symmetry does not split the degeneracy of the e-orbitals, that define the conducting properties.
55. Koehler, W. C., and Wollan, E. O. 1957, *J. Phys. Chem. Solids* 2, 100.
56. Goodenough, J. B. 1958, *J. Phys. Chem. Solids* 6, 287.
57. Raccach, P. M., and Goodenough, J. B. 1967, *Phys. Rev.* 155, 932.
58. Señaris-Rodríguez, M. A., and Goodenough, J. B. 1995, *J. Solid State Chem.* 116, 224.
59. Señaris-Rodríguez, M. A., and Goodenough, J. B. 1995, *J. Solid State Chem.* 118, 323.
60. Zhuang, M., Zhang, W., and Ming, N. 1998, *Phys. Rev. B* 57, 10705.
61. Zhuang, M., Zhang, W., Hu, C., and Ming, N. 1998, *Phys. Rev. B* 57, 10710.
62. Potze, R. H., Sawatzky, G. A., and Abbate, M. 1995, *Phys. Rev. B* 51, 11501.
63. Korotin et al. 1996, *Phys. Rev. B* 54, 5309.
64. Saitoh et al. 1997, *Phys. Rev. B* 55, 4257.
65. Yamaguchi, S., Okimoto, Y., and Tokura, Y. 1997, *Phys. Rev. B* 55, R8666.
66. Demazeau, M. Pouchard, M., and Hagenmüller, P. 1974, *J. Solid State. Chem.* 9, 202.
67. Yamaguchi, S., Taniguchi, H., Takagi, H., Arima, T., and Tokura, Y. 1995, *J. Phys. Soc. Jpn.* 64, 1885.
68. Golovanov, V., Mihaly, L., and Moodenbaugh, A. R. 1996, *Phys. Rev. B* 53, 8207.
69. Mahendiran, R., and Raychaudhuri, A. K. 1996, *Phys. Rev. B* 54, 16044.
70. Jonker, G. H., and van Santen, J. H. 1953, *Physica* 19, 120.
71. Itoh, M., Natori, I., Kubota, S., and Motoya, K. 1994, *J. Phys. Soc. Jpn.* 63, 1486.
72. Mira, J., Rivas, J., Vázquez, M., García Beneytez, J. M., Arcas, J., Sánchez, R. D., and Señaris Rodríguez, M. A. 1999, *Phys. Rev. B* 59, 123.
73. Vázquez, M., García Beneytez, J. M., Arcas, J., Castaño, F. J., Mira, J., Rivas, J., Breijo, M. P., and Señaris Rodríguez, M. A. 1999, *J. Magn. Magn. Mater.* 196-197, 546.
74. For further description of these techniques see for example Kellner, W. U., Fähnle, M., Kronmüller, H., and Kaul, S. N. 1987, *Phys. Stat. Sol. B* 144, 387.
75. Vonsovskii, S. V. 1974, *Magnetism* (Vol. 2, Chap. 25), Wiley, New York.
76. Ibarra, M. R., Mahendiran, R., Marquina, C., García Landa, B., Blasco, J. 1998, *Phys. Rev. B* 57, R3217.
77. Caciuffo, R., Mira, J., Rivas, J., Señaris-Rodríguez, M. A., Radaelli, P. G., Carsughi, F., Fiorani, D., Goodenough, J. B. 1999, *Europhys. Lett.* 45, 399.
78. Caciuffo, R., Rinaldi, D., Barucca, G., Mira, J., Rivas, J., Señaris-Rodríguez, M. A., Radaelli, P. G., Fiorani, D., Goodenough, J. B. 1999, *Phys. Rev. B* 59, 1068.
79. Fisher, M. E., Ma, S.-K., and Nickel, B. G. 1972, *Phys. Rev. Lett.* 29, 917.

80. Radaelli, P. G., Cox, D. E., Marezio, M., Cheong, S.-W., Schiffer, P. E., and Ramírez, A. P. 1995, *Phys. Rev. Lett.* 75, 4488.
81. Menyuk, N., Raccach, P. M., and Dwight, K. 1968, *Phys. Rev.* 166, 510.
82. LaCoO<sub>3</sub> presents a distorted perovskite structure. The introduction of the larger size Sr<sup>2+</sup> cations progressively reduces the rhombohedral distortion present in the parent LaCoO<sub>3</sub>. For more details see for example Ref. [59] and references therein.
83. Stanley, H. E. 1967, *Phys. Rev.* 158, 546.
84. Abbate, M., et al. 1993, *Phys. Rev. B* 47, 16124.
85. Munakata, F., Takahashi, H., Akimune, Y., Shichi, Y., Tanimura, M., Inoue, Y., Itti, R., and Koyama, Y. 1997, *Phys. Rev. B* 56, 979.
86. Mira, J., Rivas, J., Sánchez, R. D., Señaris-Rodríguez, M. A., Fiorani, D., Rinaldi, D., and Caciuffo, R. 1997, *J. Appl. Phys.* 81, 5753.
87. Gayathri, N., Raychaudhuri, A. K., Tiwary, S. K., Gundakaram, R., Arulraj, A., and Rao, C. N. R. 1997, *Phys. Rev. B* 56, 1345.
88. Poon, S. J., and Durand, J. 1977, *Phys. Rev. B* 16, 316.
89. Müller-Krumbhaar, H. 1976, *J. Phys. C* 9, 345.
90. Nam, D. N. H., Jonason, K., Nordblad, P., Khiem, N. V., and Phuc, N. X. 1999, *Phys. Rev. B* 59, 4189.